FRET-based sensor for CaMKII activity (FRESCA): A useful tool for assessing CaMKII activity in response to Ca^{2+} oscillations in live cells

Received for publication, May 7, 2019, and in revised form, June 11, 2019 Published, Papers in Press, June 14, 2019, DOI 10.1074/jbc.RA119.009235

Goli Ardestani[‡§1], **Megan C. West**[¶1], **Thomas J. Maresca**[‖], **Rafael A. Fissore**[‡], **and Margaret M. Stratton**[¶2]

From the [‡]*Department of Veterinary and Animal Sciences,* [§]*Veterinary and Animal Sciences Graduate Program, and the Departments of* [¶]*Biochemistry and Molecular Biology and* [‖]*Biology, University of Massachusetts, Amherst, Massachusetts 01003*

Edited by Roger J. Colbran

Ca^{2+} oscillations and consequent Ca^{2+}/calmodulin-dependent protein kinase II (CaMKII) activation are required for embryogenesis, as well as neuronal, immunological, and cardiac signaling. Fertilization directly results in Ca^{2+} oscillations, but the resultant pattern of CaMKII activity remains largely unclear. To address this gap, we first employed the one existing biosensor for CaMKII activation. This sensor, Camui, comprises CaMKIIα and therefore solely reports on the activation of this CaMKII variant. Additionally, to detect the activity of all endogenous CaMKII variants simultaneously, we constructed a substrate-based sensor for CaMKII activity, FRESCA (FRET-based sensor for CaMKII activity). To examine the differential responses of the Camui and FRESCA sensors, we used several approaches to stimulate Ca^{2+} release in mouse eggs, including addition of phospholipase Cζ cRNA, which mimics natural fertilization. We found that the Camui response is delayed or terminates earlier than the FRESCA response. FRESCA enables assessment of endogenous CaMKII activity in real-time by both fertilization and artificial reagents, such as Sr^{2+}, which also leads to CaMKII activation. FRESCA's broad utility will be important for optimizing artificial CaMKII activation for clinical use to manage infertility. Moreover, FRESCA provides a new view on CaMKII activity, and its application in additional biological systems may reveal new signaling paradigms in eggs, as well as in neurons, cardiomyocytes, immune cells, and other CaMKII-expressing cells.

Calcium is a crucial ubiquitous second messenger in the cell. All electrically coupled cells, such as neurons and cardiomyocytes, and even cells that are not, such as lymphocytes and oocytes/eggs, communicate or are induced to differentiate following intracellular Ca^{2+} changes caused by Ca^{2+} release and/or Ca^{2+} influx through channels whose combined output can result in a single Ca^{2+} rise or in more complex responses such as oscillations (1–4). Absence of Ca^{2+} signals lead to severe defects in cell functionality, such as memory deficits in the case of neurons (5), or in the case of eggs, failure of fertilization and initiation of embryo development (6, 7).

In oocytes, and other cell types, Ca^{2+}/calmodulin-dependent protein kinase II (CaMKII)[3] is responsible for reacting to Ca^{2+} increases and transducing this signal to downstream molecules. Indeed, it has been shown that neuronal CaMKII has a threshold frequency for activation (8, 9). CaMKII has a unique oligomeric structure among the protein kinase family (Fig. 1*A*). Each subunit of CaMKII is comprised of a kinase domain, a regulatory segment, a variable linker region, and a hub domain (Fig. 1*B*). The hub domain is responsible for oligomerization, which organizes it into two stacked hexameric (or heptameric) rings to form a dodecameric (or tetradecameric) holoenzyme (8, 10, 11). In the absence of Ca^{2+}, the regulatory segment binds to and blocks the substrate-binding pocket. Ca^{2+}/calmodulin (Ca^{2+}/CaM) turns CaMKII on by competitively binding the regulatory segment and exposing the substrate-binding pocket (Fig. 1*C*). Unlike other Ca^{2+}/CaM-sensitive kinases, CaMKII acquires activity that is Ca^{2+} independent (autonomy) with sustained stimulation by autophosphorylation at Thr-286 (we will use CaMKIIα numbering throughout the manuscript) (Fig. 1*C*) (12, 13). In other words, as long as Thr-286 is phosphorylated, CaMKII will retain activity, even in the absence of Ca^{2+}. It is this property, combined with its oligomeric organization, which provides the sensitivity of CaMKII to specific frequencies of Ca^{2+} rises.

CaMKII is essential for oocyte activation and initiation of embryo development (Fig. 1*D*). All vertebrate oocytes are arrested at the time of fertilization at the metaphase (M) stage of meiosis II (MII); henceforth referred to as eggs. This arrest is underpinned by a complex regulation of the activity of the maturation-promoting factor, which is maintained high during the arrest (14, 15). Maturation-promoting factor inactivation is required to complete meiosis and initiate the mitotic cycles of early embryogenesis. A prolonged Ca^{2+} signal, in the form of multiple oscillations, is initiated by the sperm and is responsible for inducing the release of the meiotic arrest at fertilization in

This work was supported by the University of Massachusetts, Amherst, and National Institutes of Health, NIGMS Grant 5R01GM123157 (to M. M. S.) and NICHD Grants HD051872 and HD092499 (to R. A. F.). The authors declare that they have no conflicts of interest with the contents of this article. The content is solely the responsibility of the authors and does not necessarily represent the official views of the National Institutes of Health.
This article contains Figs. S1–S9.

[1] Both authors contributed equally to the results of this article.

[2] To whom correspondence should be addressed. Tel.: 413-545-0631; E-mail: mstratton@biochem.umass.edu.

[3] The abbreviations used are: CaMKII, Ca^{2+}/calmodulin-dependent protein kinase II; FRESCA, FRET-based sensor for CaMKII activity; PKC, protein kinase C; MII, metaphase II; PLC ζ1, phospholipase C ζ1; PMA, phorbol 12-myristate 13-acetate; CFY, cyan fluorescent protein; YFP, yellow fluorescent protein; ANOVA, analysis of variance.

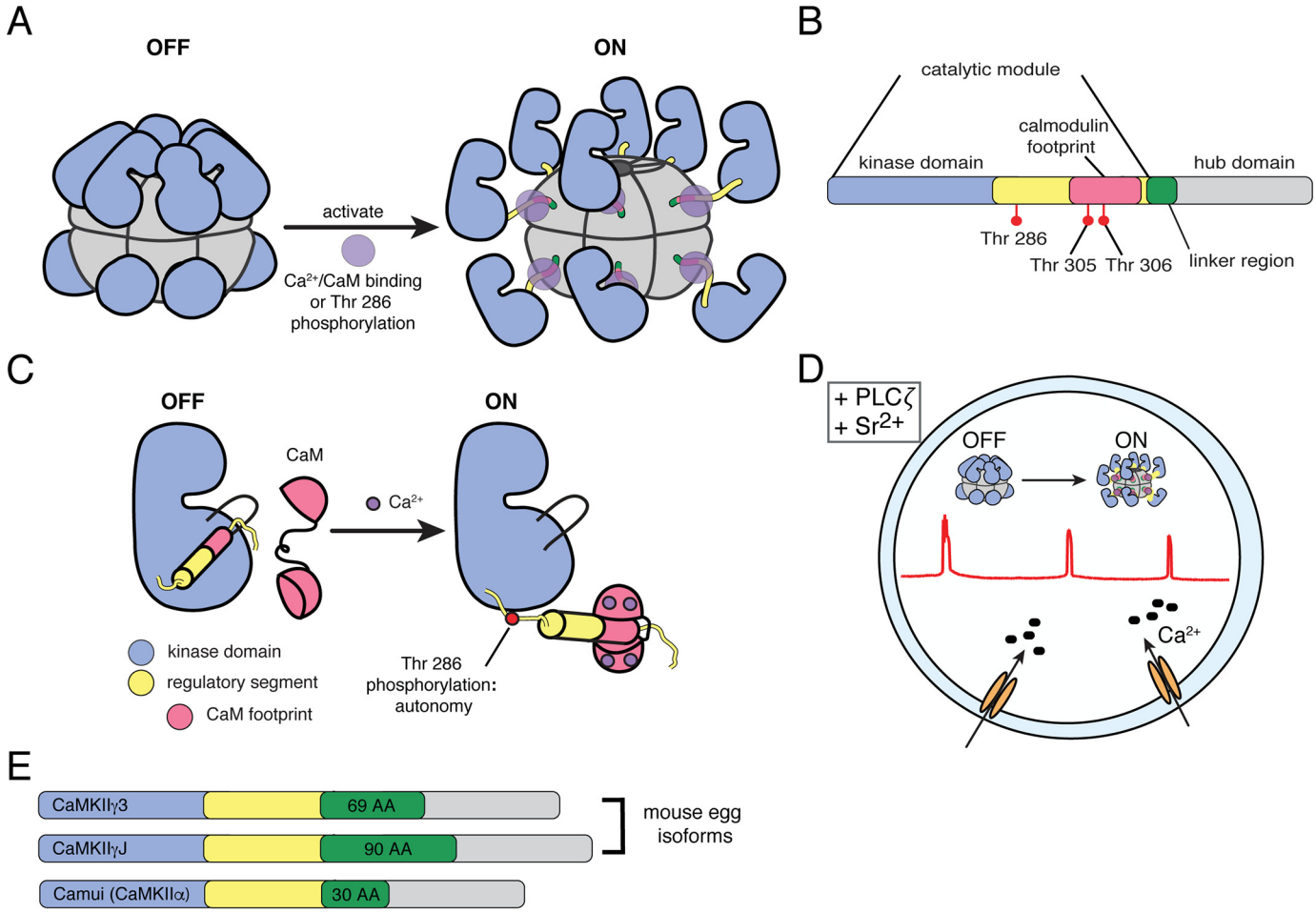

Figure 1. CaMKII: an essential enzyme. *A*, CaMKII is an oligomeric complex turned on by Ca^{2+}/CaM binding, which facilitates autophosphorylation at Thr-286. *B*, each CaMKII subunit is comprised of a kinase domain, regulatory segment, which houses the Ca^{2+}/CaM-binding domain, a variable linker region, and a hub domain. Herein, we use the numbering for CaMKIIα. *C*, the regulatory segment of CaMKII maintains its off state in the absence of calcium by blocking its substrate-binding pocket. Ca^{2+}/CaM competes with the regulatory segment, thereby activating the kinase and allowing for Thr-286 phosphorylation, which yields autonomous activity. Even when the calcium stimulus diminishes, CaMKII stays on as long as Thr-286 is phosphorylated. *D*, in mammalian eggs, addition of PLCζ or Sr^{2+} leads to stimulation of calcium oscillations and CaMKII activation. CaMKII is expected to be "off" in the absence of Ca^{2+} and turn "on" after Ca^{2+} levels rise. *E*, linear sequences of the two CaMKII isoforms reported in eggs (CaMKII γ3 and γJ) and Camui (CaMKIIα). Color codes are the same as in *B*, the CaM footprint has been removed for clarity.

all mammals, as preventing their generation results in failure of MII exit (16). Importantly, Ducibella *et al.* (17) showed that these Ca^{2+} oscillations are not redundant, rather, several Ca^{2+} rises are required for the early signaling events essential for embryogenesis. Indeed, it has been hypothesized that these early Ca^{2+} signals also play a role in long-term signaling in the developing embryo (17, 18).

It was first shown in *Xenopus* eggs that the Ca^{2+} rise induced by the sperm resulted in CaMKII activation, which is required for the initiation of embryogenesis (19). In mammals, this was demonstrated using genetic models where CaMKII was knocked-out and/or down-regulated, which resulted in sterile females despite the ability of their eggs to initiate normal Ca^{2+} oscillations. These studies confirmed the requirement of CaMKII for the initiation of mammalian embryo development (20, 21). Despite these findings, the complete profile of CaMKII activity during fertilization in mammals is not known. Using *in vitro* kinase assays and egg lysates, an elegant series of papers showed that these early Ca^{2+} rises induced CaMKII activity corresponding with discrete Ca^{2+} rises during the first hour post-fertilization (17, 18, 22, 23). Nevertheless, Ca^{2+} rises associated with fertilization in mammalian species occur every ~20 min and last longer than 3 h, and the changes in CaMKII activity associated with all oscillations have not been determined.

In mammalian eggs, the Ca^{2+} oscillations induced by fertilization that activate CaMKII and promote egg activation occur with characteristic amplitude and frequency (24, 25). Interestingly, it has been shown that CaMKII has a threshold frequency for activation (8, 9). There are four human CaMKII genes: CaMKIIα and -β are predominantly found in the brain, CaMKIIδ is found in the heart, and CaMKIIγ is found in multiple organ systems, including the reproductive organs. The kinase and hub domains of all four genes are highly conserved (~95 and 80% identity, respectively), however, the linker connecting the kinase and hub domains is highly variable in length and composition (see Fig. 1*B*). Details elucidating the importance of the variable linker region remain to be uncovered, but there are several splice variants of each of the four genes, which mostly vary in the linker region. It has been shown that CaMKII activity is tuned by the length of the variable linker (8). Specif-

ically, as the variable linker is lengthened, less Ca^{2+} is needed for activation (*i.e.* activation of CaMKII is easier). Mouse eggs express equimolar concentrations of the two versions of CaMKIIγ (γ3 and γJ, Fig. 1*E*) (26). The underlying regulation and contributions of these isoforms in mammalian eggs has not been investigated.

To date, CaMKII activity has only been assessed based on a few Ca^{2+} rises using *in vitro* kinase assays and during only the first hour of oscillations, which is considerably shorter than the time scale for normal oscillations in the mouse. Therefore, there is a need to monitor CaMKII activity in live cells and for an extended time, which is what we address here.

Results

Measuring CaMKII activity in real-time in mouse eggs

Herein, we show CaMKII activity monitored in real-time following the induction of Ca^{2+} responses using several agonists that are capable of initiating embryogenesis. To examine the real-time changes, we expressed the Camui reporter (see Fig. 2*A*) in mouse eggs. Camui is a Förster resonance energy transfer (FRET)-based biosensor for CaMKII activity, which exploits the conformational change that CaMKII undergoes when it binds to Ca^{2+}/CaM (27) (Fig. 2*A*). Camui is currently the only biosensor for CaMKIIα activity. Camui expression was robust about ~30 min after cRNA injection, and monitoring was performed 3 h post-injection to attain reasonably stable Camui levels. We first examined the distribution of Camui using confocal microscopy and observed widespread cytoplasmic expression (Fig. 2*B*).

Camui monitoring of ionomycin-induced Ca^{2+} rises

Given the immediate and large Ca^{2+} rise caused by the addition of ionomycin, we first tested Camui responses in eggs using this ionophore. We analyzed the effect of 3 concentrations of ionomycin: 0.5, 2.5, and 5 μM. Upon addition of ionomycin to eggs expressing Camui, we observed a decrease in ratiometric FRET (YFP/CFP), indicating CaMKII activation (Fig. 2, *C–E*). As expected with a decrease in FRET, we observed a corresponding increase in CFP fluorescence and decrease in YFP fluorescence (Fig. S3*B*).

It is clear that CaMKII activity increases (red line) coincident with the increase in Ca^{2+} (black line) in all conditions. The Ca^{2+} and Camui responses increased dose-dependently and approximately synchronously, as the large increase in the amount of Ca^{2+} release caused by increasing ionomycin from 0.5 to 2.5 μM, results in a 1.9-fold increase in CaMKII activity (mean amplitude of FRET change) (Fig. 2*F*). Further increasing ionomycin from 2.5 to 5 μM produces nearly no change in total Ca^{2+} release, although it is very likely that the reporting range of Rhod-2 is saturated at these levels of intracellular Ca^{2+}. The CaMKII activity also appears to remain constant, although this may also represent saturation of the FRET signal (Fig. 2*F*). Notably, addition of 5 μM ionomycin results in a faster and prolonged duration of activity compared with lower concentrations (Fig. 2*G*), but it is unclear whether this reflects the extended activation of the enzyme or cellular stress.

Camui monitoring of Sr^{2+}-induced oscillations

We next examined the Camui response to Sr^{2+}-induced oscillations (Fig. 3). Addition of 10 mM Sr^{2+} to the extracellular media in place of external Ca^{2+} is a common method of parthenogenetic activation in mouse eggs. Also, 10 mM Sr^{2+} induces highly consistent oscillations in these cells (Fig. 3, *black lines*); these oscillations initiate all events of egg activation (28–30). The TRPV3 channel has recently been identified as the channel responsible for Sr^{2+} influx in mouse eggs (30). These oscillations, as reported by Rhod-2 in the following experiments, are most likely to represent a combination of both Ca^{2+} and Sr^{2+} release, with a progressively greater release of Sr^{2+} as these measurements were performed in the absence of extracellular Ca^{2+}. Camui reported FRET changes following the initiation of oscillations by Sr^{2+} (Fig. 3, *red lines*). Remarkably, the FRET changes were delayed, despite the presence of robust changes in intracellular Ca^{2+}/Sr^{2+} levels. Roughly 82% of eggs (14/17) did not report significant CaMKII activity until the ~4th Ca^{2+}/Sr^{2+} rise, where some initial activity is seen at the 3rd rise (Fig. 3*B*, *arrow* and *inset*). In a few eggs (2/10), we observed longer delays, until the 5th rise (Fig. S1).

Another distinctive feature of the Camui response caused by Sr^{2+} oscillations is that although the initial Camui responses were delayed, once they commenced, they displayed an integrated activation with each subsequent pulse during the first few pulses. We analyzed the mean amplitude for the first three observable FRET changes. From the first to the second FRET change, there was a 1.6-fold increase in CaMKII activity. From the second to the third FRET change, there was a negligible change, and these changes occurred while the amplitude of the Ca^{2+} peaks progressively decreased and/or remained unchanged (Fig. 3, *C–E*). These data indicate that CaMKII activity, once stimulated by Ca^{2+}/Sr^{2+} rises, is cooperative in response to the initial rises until saturation is achieved, which is around the 3rd FRET response. This result is consistent with previous data showing that CaMKII activity is highly cooperative *in vitro* (8, 31). As depicted in Fig. 3*A*, a potential explanation for this is phosphorylation at Thr-286, which may persist even in the absence of elevated Ca^{2+}. It has been clearly shown that CaMKII with Thr-286 phosphorylated has a significantly higher affinity for Ca^{2+}/CaM (32). This would also explain why individual FRET responses outlasts individual Ca^{2+} rises and do not return to baseline simultaneously (Fig. 3*B*, Fig. S1, *blue horizontal lines*).

Considerations for endogenous CaMKII in eggs

To date, Camui has been a useful tool to study and understand CaMKII activity in various cell types and under various conditions. Despite the many insights gained by the widespread use of Camui, it is an over-expressed protein reporter construct and it does not necessarily faithfully report the activation state of endogenous CaMKII in any cell. Camui had not been used to monitor CaMKII activity in mouse eggs until this study. Because the Camui sensor is constructed of a CaMKII variant itself, it will report on this particular variant, in this case is CaMKIIα with a 30-residue linker region, which is not expressed in mammalian eggs (see Fig. 1*E*). Given that it has

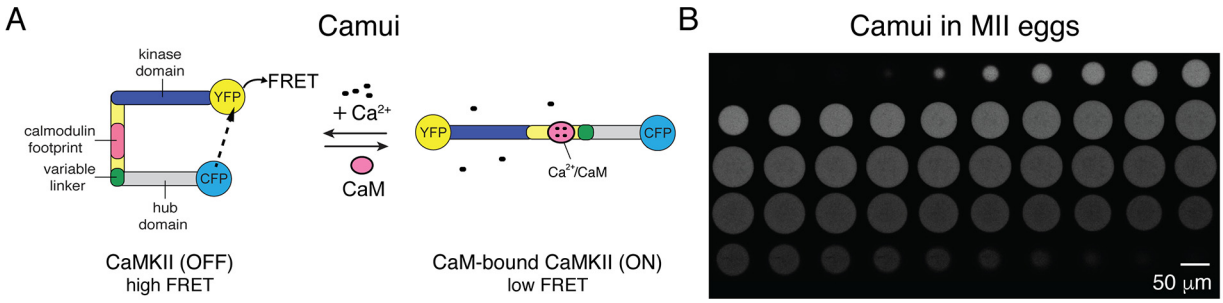

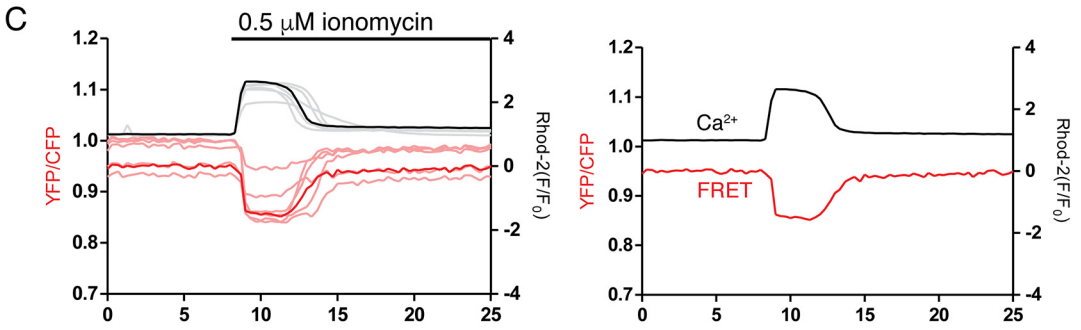

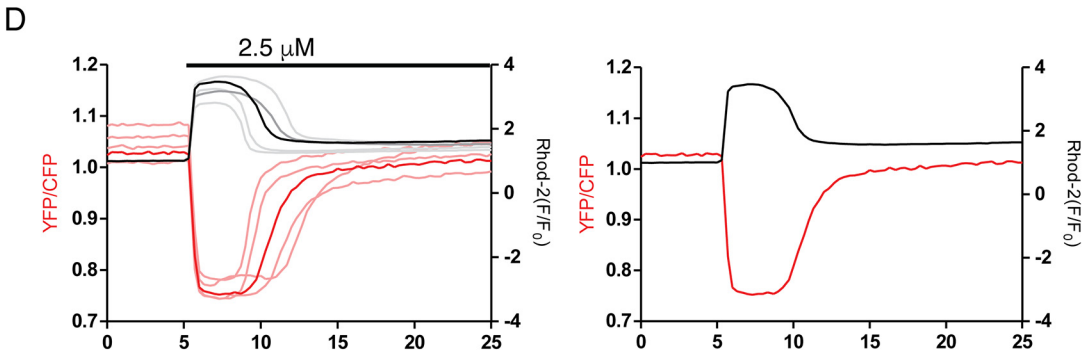

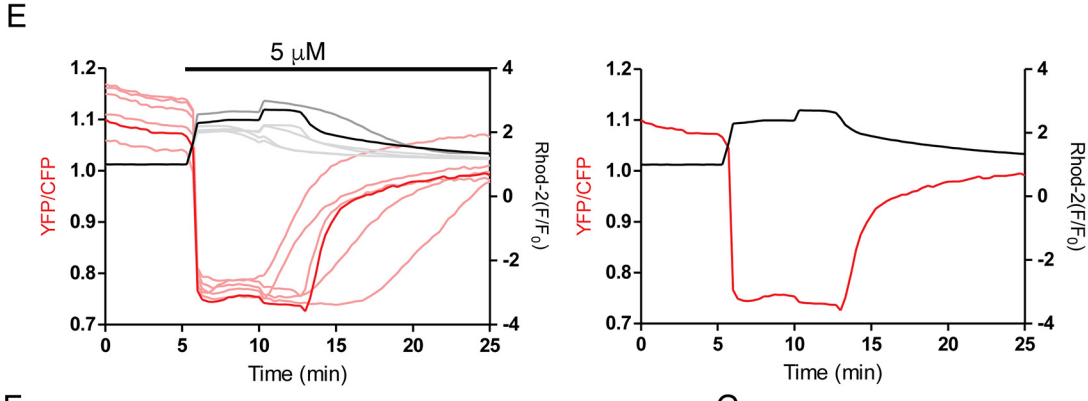

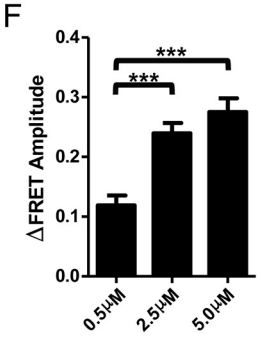

	0.5μM	2.5μM	5.0μM
Mean	0.1187	0.2394	0.2750
Std. Deviation	0.0675	0.07825	0.06573
Std. Error	0.01689	0.01750	0.02324

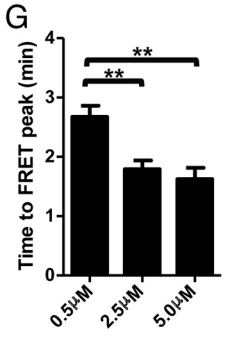

	0.5μM	2.5μM	5.0μM
Mean	2.675	1.790	1.625
Std. Deviation	0.6426	0.6088	0.5418
Std. Error	0.1855	0.1477	0.1916

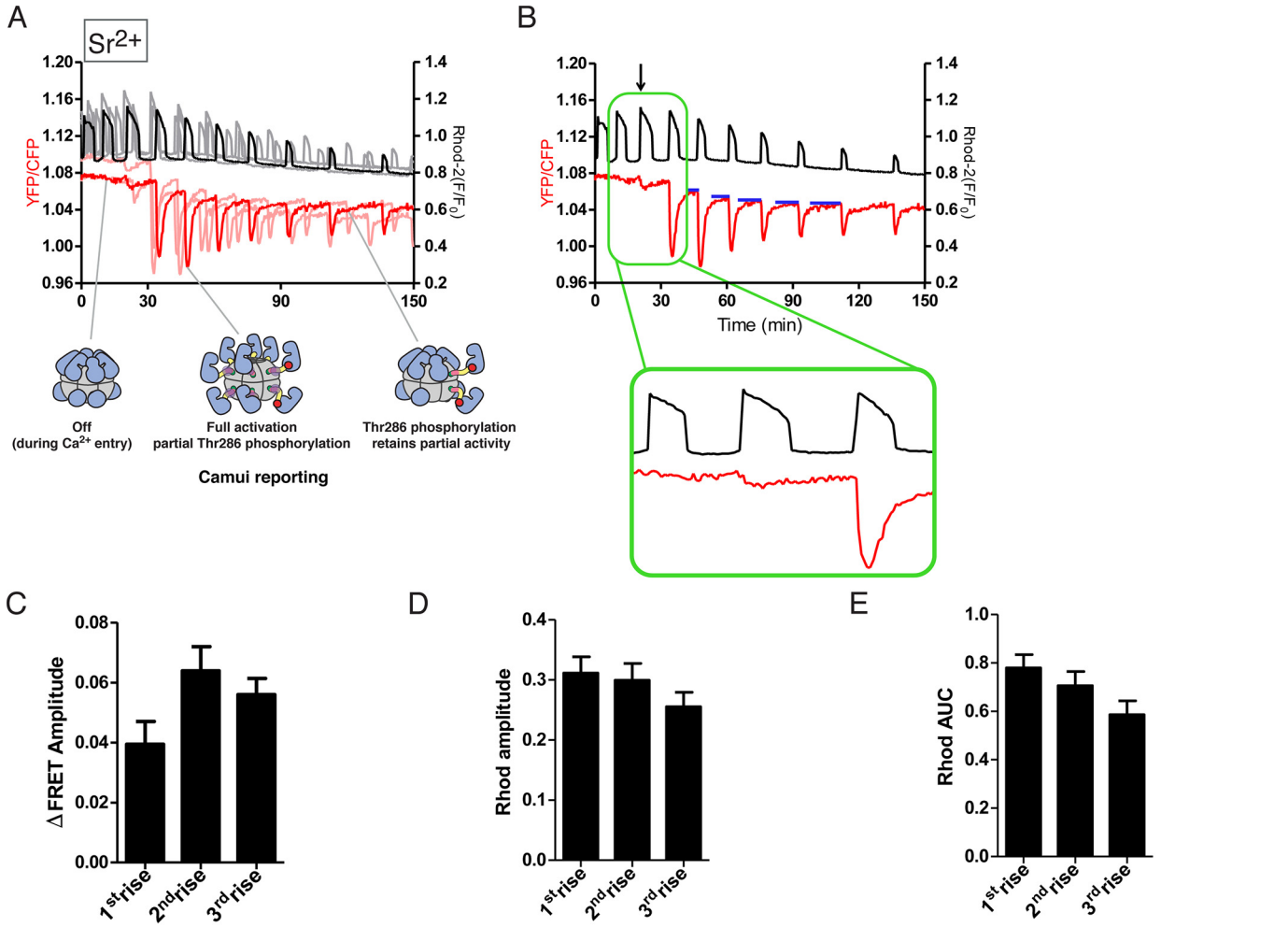

	1st rise	2nd rise	3rd rise
Mean	0.03941	0.06391	0.05598
Std. Deviation	0.02954	0.03024	0.02020
Std. Error	0.007627	0.008082	0.005400

	1st rise	2nd rise	3rd rise
Mean	0.3115	0.2994	0.2556
Std. Deviation	0.1048	0.1046	0.09001
Std. Error	0.02706	0.02796	0.02406

	1st rise	2nd rise	3rd rise
Mean	0.7793	0.7063	0.5860
Std. Deviation	0.2128	0.2179	0.2149
Std. Error	0.05494	0.05822	0.05743

Figure 3. Camui activity tracks Ca^{2+} oscillations in mouse eggs in a delayed manner. *A*, Ca^{2+}/Sr^{2+} oscillations are induced by addition of 10 mM Sr^{2+}. Ca^{2+} is monitored by Rhod-2 (*black line*) and CaMKII activity is tracked by Camui (*red line*). CaMKII cartoons indicate hypothesized molecular details during the Ca^{2+} pulses. *B*, one representative trace from Sr^{2+} oscillations is shown. *Blue lines* indicate baseline CaMKII activity after each rise. *Arrow* indicates first significant FRET response. *C–E*, three Ca^{2+} rises were quantified. The "1st rise" is that which induced the first FRET response, and then the subsequent 2 rises were measured. The ΔFRET amplitude (*C*), rhodamine amplitude (*D*), and rhodamine area under the curve (*E*) are shown. Statistics are reported in the adjacent tables. 15 eggs over 3 replicates were used to generate the statistics.

been demonstrated that CaMKII activity is tuned by the length of the variable linker (8, 33), specifically, as the variable linker is lengthened, less Ca^{2+} is needed for activation, we hypothesized that Camui may not be reporting faithfully on the endogenous CaMKII in eggs. This assumption is based on the knowledge that mouse eggs express, as mentioned, equimolar concentrations of the two versions of CaMKIIγ (γ3 and γJ), which have 69- and 90-residue variable linkers, respectively (Fig. 1*E*) (34), considerably longer than the 30-residue linker of CaMKIIα. We suspected this might be the case because of the lack of FRET changes following the initial large changes in Rhod-2 fluorescence induced by Sr^{2+} oscillations. This possible limitation of the Camui reporter led us to seek additional methods to detect these physiological changes. One option is to re-engineer

Figure 2. Simultaneously monitoring Ca^{2+} influx and CaMKII activity using Camui. *A*, Camui is an existing biosensor for CaMKII activity, which exploits the conformational change of CaMKII binding to Ca^{2+}/CaM to report on activity using FRET. *B*, Camui expression in mouse MII eggs shows a widespread cytoplasmic distribution. Z-stacks images were collected at 1024 × 1024 in 12 bits and the step size was 1.00 μm. *Scale bar* is equivalent to 50 μm. *C–E*, changes in Ca^{2+} are monitored using Rhod-2 (*black*) and CaMKII activity is monitored using Camui (*red*). Multiple traces are shown after 0.5 (*C*), 2.5 (*D*), or 5 μM (*E*) ionomycin is added. One representative trace is shown to the *right* of each plot. *F* and *G*, quantification of Camui response to ionomycin addition. *F*, ΔFRET amplitude indicates the overall change in FRET during the duration of the Ca^{2+} signal. *G*, time to FRET peak indicates how long it takes Camui to reach maximum ΔFRET signal after addition of ionomycin and increase in Ca^{2+}. Statistics are reported in the adjacent tables, differences were considered significant at $p < 0.05$ (*) using one-way ANOVA. Post hoc analyses were done using a Tukey multiple comparison test (Prism GraphPad). Number of eggs/replicates for each condition is as follows: 0.5 μM ionomycin, 16/4; 2.5 μM ionomycin, 21/5; 5 μM ionomycin, 10/3.

Camui with the appropriate CaMKII isoform to be studied, however, this becomes cumbersome because there are multiple isoforms expressed in a single cell type. To circumvent this problem, we report here the development of a novel biosensor that detects endogenous CaMKII activity in mouse eggs.

Development of a novel biosensor for endogenous CaMKII activity

We developed a novel substrate-based sensor for CaMKII activity, FRESCA (FRET based sensor for CaMKII activity, Fig. 4*A*) and monitored CaMKII activity using FRESCA in real-time. We adapted the FRESCA design from an original design for a protein kinase C (PKC) biosensor (CKAR) from Newton and colleagues (35), which has also been adapted to make an Aurora kinase biosensor (36). The premise for this design is to engineer in a conformational change upon phosphorylation of the substrate. Cleverly, this was done by fusing the kinase substrate to a phosphate-binding protein (FHA2) (35). FHA2 will bind to this phosphorylated Thr residue and produce a decrease in FRET between the terminal CFP/YFP pair (which in this case is Turquoise and Venus, termed CFP/YFP throughout for simplicity). We cloned in a CaMKII-specific substrate (syntide-2) (37), with a few modifications to provide a better substrate for FHA2 (see "Experimental procedures" for sequence details). We refer to this peptide as syntide-FRESCA throughout for clarity.

Measuring the FRESCA response in HEK293T cells

We first tested FRESCA in HEK293T cells, which express negligible levels of CaMKII. We transfected HEK293T cells with either (i) CaMKII, calmodulin, and FRESCA, or (ii) calmodulin and FRESCA. Ionomycin was added to the HEK293T cells to induce Ca^{2+} release and simultaneously monitored FRET (YFP/CFP). We observed that with CaMKII transfected, the addition of ionomycin causes a reduction in FRET, indicating that CaMKII is active and phosphorylating FRESCA (Fig. S2, *red lines*). Importantly, we did not observe a FRET change when CaMKII was not co-transfected, demonstrating that FRESCA is selective for the transfected CaMKII and is not being phosphorylated by any intrinsic HEK cell kinases under these conditions (Fig. S2, *blue lines*).

FRESCA monitoring of ionomycin-induced Ca^{2+} release in mouse eggs

We expressed FRESCA in mouse eggs to measure endogenous CaMKIIγ activity. FRESCA expression in MII eggs resulted in uniform distribution throughout the cytoplasm (Fig. 4*B*). Upon addition of ionomycin to eggs expressing FRESCA, we observed a FRET decrease indicating CaMKII activity (Fig. 4, *C–E*). The amplitude change is 10-fold less than what is observed for Camui (0.016 for FRESCA compared with 0.16 for Camui), however, this measurable signal change is sufficient for us to monitor endogenous CaMKIIγ activity compared with the CaMKIIα of Camui. It is worth noting that the shape of the FRESCA trace is slightly different from that of Camui for the same stimulus. At the lowest ionomycin concentration (0.5 μM), CaMKII activity appears to perfectly track the Ca^{2+} rise (Fig. 4*C*). Conversely, at higher ionomycin concentrations, CaMKII activity is unstable during the duration of the Ca^{2+} rise, although higher concentrations appear to prolong and increase the FRET response of FRESCA (Fig. 4*F*). The time to FRET peak was faster with addition of higher ionomycin concentrations (Fig. 4*G*).

To demonstrate that the changes in FRESCA fluorescence reflect FRET, we plotted the traces of CFP and YFP fluorescence after the addition of ionomycin independently. As expected, the values changed simultaneously but in opposite directions (Fig. S3*A*). We also expressed YFP cRNA alone and monitored fluorescence changes following stimulation with Sr^{2+} oscillations. Consistent with the evidence that the changes in FRESCA are the result of FRET, the oscillations did not induce changes in YFP fluorescence corresponding with each Ca^{2+}/Sr^{2+} elevation (Fig. S4).

Specificity of FRESCA in mouse eggs

We sought to show that FRESCA is reporting specifically on CaMKII in eggs as opposed to other CaM kinases or Ca^{2+}-sensitive kinases. A previous study using real-time PCR revealed that transcript levels of CaMKIV were ~1% compared with those of CaMKIIγ, the predominant isoform in mouse eggs (38). Additionally, even when overexpressed, CaMKIV was insufficient to lead to egg activation. In this same study, CaMKI levels were undetectable, and CaMKK seems to also be absent in mouse eggs. There has also been a comprehensive MS study of total proteins expressed in GV oocytes and MII eggs (39). Similar to the mRNA sequencing, they detected no CaMKI and very low levels of CaMKIV. There is also no evidence for CaMKK or PKA detected in MII eggs in this study, which is indicative of low expression levels in these cells. Finally, it has not been shown that Akt or PKA undergo immediate activation following increases in intracellular Ca^{2+} rises.

We therefore focused our efforts on CaMKII and PKC, which is also a Ca^{2+}-sensitive kinase in eggs (38, 39). To this end, we compared the rates of phosphorylation of FRESCA-syntide and syntide-2 by CaMKII and PKC *in vitro* (Fig. S5). Consistent with existing data (37), we observed that CaMKII phosphorylates syntide-2 at a 3-fold higher rate compared with PKC at high substrate concentrations (0.3 mM). We next tested our new syntide variant, FRESCA-syntide. Importantly, we observe a large increase in specificity with CaMKII phosphorylating FRESCA-syntide at a 44-fold higher rate compared with PKC.

We next performed a series of experiments testing CaMKII and PKC inhibitors, and a PKC activator. CaMKII inhibitors should eliminate the FRET response if CaMKII is the only kinase phosphorylating FRESCA in eggs. We show that the addition AS105, a CaMKII-specific ATP competitive inhibitor, significantly reduced FRET, whereas its inactive analog (AS461) did not affect FRET (Fig. 5*A*) (40). It is important to note that we also tested a common CaMKII inhibitor, KN93, which significantly reduced the amount of Ca^{2+} released upon addition of ionomycin (41) (data not shown). In addition to the recent study that showed KN93 binds Ca^{2+}/CaM (42), we chose to not pursue this inhibitor further.

We next tested the PKC inhibitor GO6983 (43), which did not affect the FRESCA signal, indicating that PKC is not phosphorylating FRESCA, which is consistent with our *in vitro*

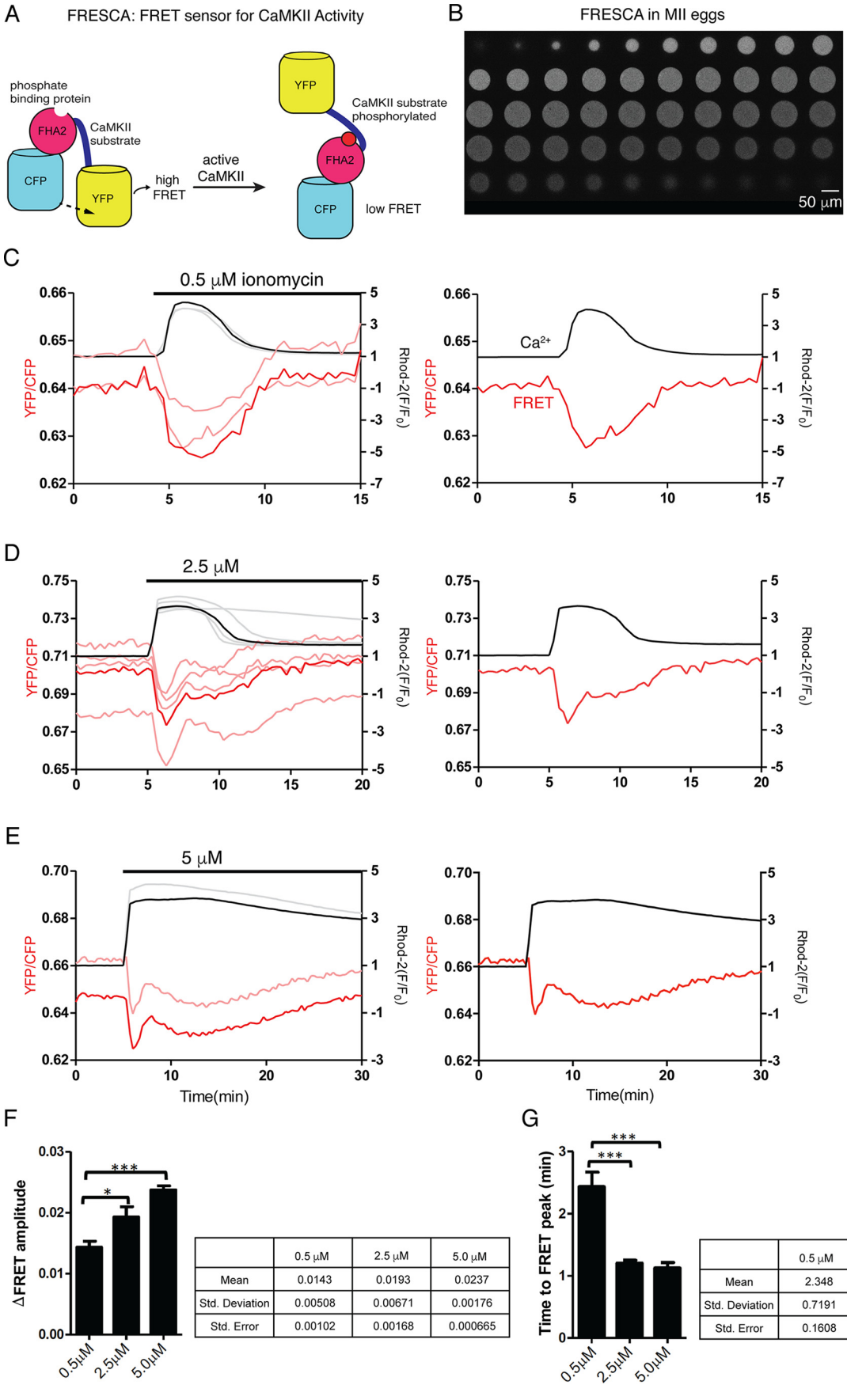

	0.5 μM	2.5 μM	5.0 μM
Mean	0.0143	0.0193	0.0237
Std. Deviation	0.00508	0.00671	0.00176
Std. Error	0.00102	0.00168	0.000665

	0.5 μM	2.5 μM	5.0 μM
Mean	2.348	1.206	1.125
Std. Deviation	0.7191	0.1806	0.2480
Std. Error	0.1608	0.04516	0.08768

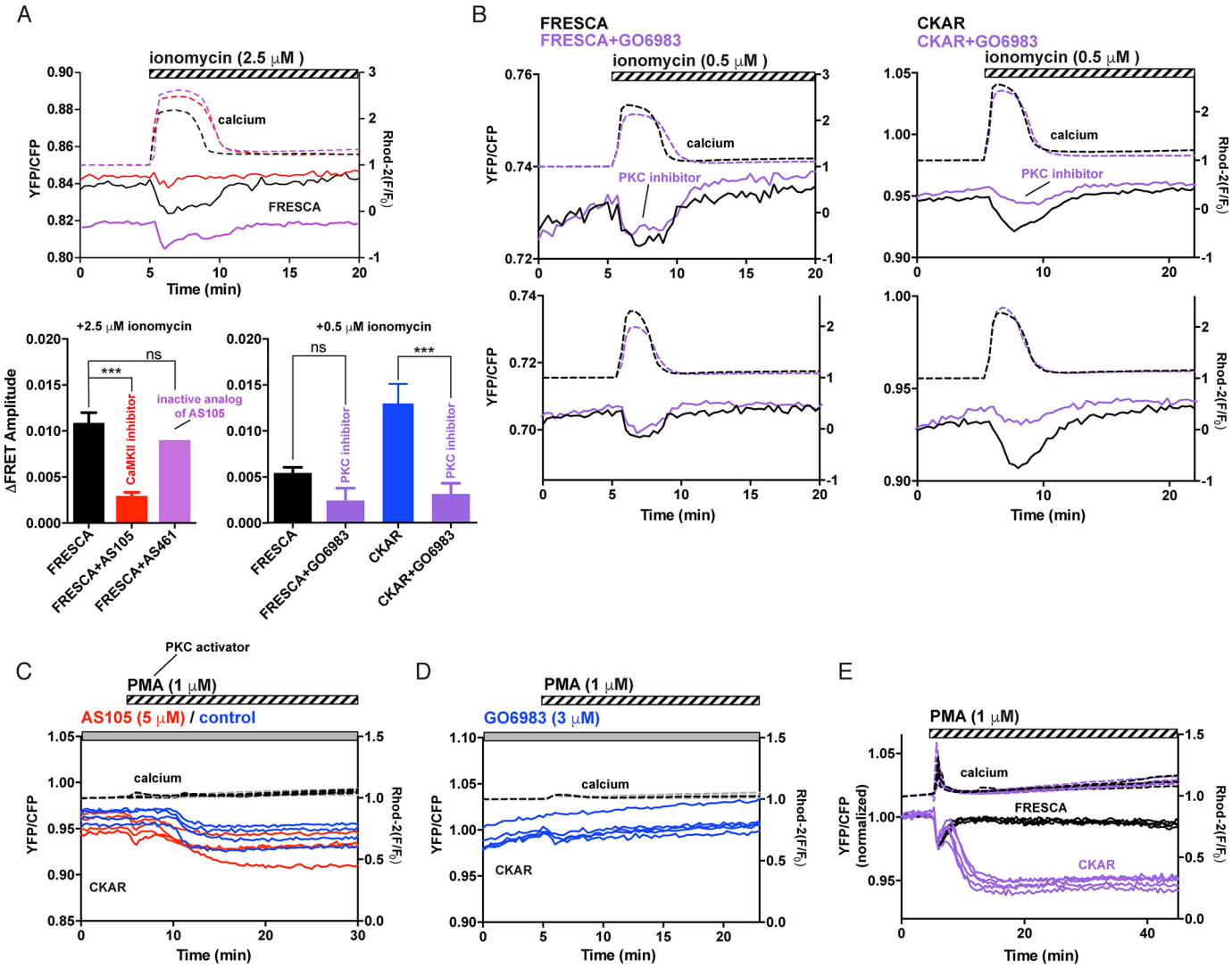

Figure 5. FRESCA specificity in mouse eggs. Various compounds were added to mouse eggs expressing FRESCA and CKAR. In all, Ca^{2+} was monitored using Rhod-2 (*hashed lines*) and FRET was monitored by YFP/CFP ratio (*solid lines*). Colors correspond to the labeled bar graph. The *bar graphs below* show the quantification of the plots in *A* and *B*, where the values were corrected by subtracting the fluorescence from noninjected controls. Differences were considered significant at $p < 0.05$ (*) using one-way ANOVA comparing the 2.5 μM ionomycin data and 0.5 μM ionomycin data in separate analyses. Post hoc analyses were done using a Tukey multiple comparison test (Prism GraphPad). *A*, CaMKII inhibitor: AS105 (5 μM) and inactive analog of this inhibitor, AS461 (5 μM), were added to mouse eggs and stimulated with 2.5 μM ionomycin. *B*, PKC inhibitor: GO6983 (5 μM) was added to mouse eggs expressing either FRESCA or CKAR and stimulated with 0.5 μM ionomycin. These were directly compared with FRESCA and CKAR alone and a noninjected control with 0.5 μM ionomycin. *C*, a PKC-specific activator: PMA (1 μM) was added to mouse eggs expressing CKAR, with or without the addition of the CaMKII inhibitor AS105 or GO6983 (*D*). *E*, PMA is added to eggs expressing FRESCA or CKAR. FRET values were normalized to 1.0 for comparison. Number of eggs used in each condition is reported under "Experimental procedures."

kinetic data (Fig. 5*B*, Fig. S5). Eggs do not express conventional PKC isoforms, which is why we chose to use the broad-spectrum PKC inhibitor (GO6983). To ensure that PKC in our system is responding to these agents, we measured the PKC response directly using the CKAR biosensor for PKC activity (35). The phorbol ester, PMA, has been shown to activate PKC in the absence of a Ca^{2+} stimulus (44), which we also observed (Fig. 5, *C* and *E*). The CaMKII inhibitor AS105 does not affect the CKAR response to PMA at all (Fig. 5*C*), but GO6983 completely abolishes the CKAR response (Fig. 5*D*). Compared side-by-side, PMA strongly and persistently activates CKAR but not FRESCA (Fig. 5*E*). We note a transient rise in Ca^{2+} upon PMA

Figure 4. Monitoring endogenous CaMKII activity using FRESCA. *A*, a cartoon of a substrate-based CaMKII biosensor is shown: FRESCA. Active CaMKII phosphorylates its substrate (syntide), which then acts as a substrate for FHA2 (phosphate-binding domain). This induces a conformational change in the sensor as a consequence of CaMKII activity. *B*, confocal image of FRESCA expression in a mouse MII egg. Z-stacks images were collected at 1024 × 1024 in 12 bits and the step size was 1.00 μm. *Scale bar* is equivalent to 50 μm. *C–E*, changes in Ca^{2+} are monitored using Rhod-2 (*black*) and CaMKII activity is monitored using FRESCA (*red*). Multiple traces are shown after 0.5 (*C*), 2.5 (*D*), or 5 μM (*E*) ionomycin is added. One representative trace is shown to the *right* of each plot. *F* and *G*, quantification of FRESCA response to ionomycin addition. ΔFRET amplitude (*F*) indicates the overall change in FRET during the duration of the Ca^{2+} signal. Time to FRET peak (*G*) indicates how long it takes FRESCA to reach maximum ΔFRET signal after addition of ionomycin and increase in Ca^{2+}. Statistics are reported in the adjacent tables, differences were considered significant at $p < 0.05$ (*) using one-way ANOVA. Post hoc analyses were done using a Tukey multiple comparison test (Prism GraphPad). Number of eggs/replicates for each condition is as follows: 0.5 μM ionomycin, 13/4; 2.5 μM ionomycin, 21/5; 5 μM ionomycin, 8/3.

addition, during which we also see a corresponding transient FRET response in both CKAR and FRESCA. The FRESCA FRET response immediately returns to baseline, whereas the CKAR FRET change continues to decrease, indicating persistent activation. There is previous evidence showing changes in Ca^{2+} upon addition of phorbol ester compounds, to which this is attributed (45).

Finally, we closely compared the response dynamics of Camui, FRESCA, and CKAR in response to ionomycin addition (Fig. S6). It is clear that both Camui and FRESCA show the same response pattern, where the FRET response essentially mirrors the Ca^{2+} rise. When this is directly compared with CKAR, it is clear that CKAR has a delayed response, and maximal activity is not coincident with maximum Ca^{2+}. This observation is in line with previous studies using CKAR to monitor PKC activity in eggs (46). Taken all together, we show that FRESCA is specifically reporting on endogenous CaMKII activity in the egg.

FRESCA monitoring of Sr^{2+}-induced Ca^{2+} oscillations

Next, we examined the response of endogenous CaMKII to Sr^{2+}-induced oscillations (Fig. 6). We observed endogenous CaMKIIγ activity (monitored by FRESCA) almost simultaneously with the initiation of oscillations. Indeed, over 70% of eggs (8/11) showed CaMKII activity with the first Ca^{2+} rise. The other 3 eggs responded at the second Ca^{2+} rise. Importantly, CaMKII activity is prolonged over time, as FRESCA continues to track each Ca^{2+} rise for >2 h (Fig. 6, *A* and *B*). In contrast, only 18% of the eggs (3/17) expressing Camui showed activity during the first Ca^{2+} rise.

We tested the effect of the PKC inhibitor GO6983 on both FRESCA and CKAR in response to Sr^{2+}-induced oscillations. In this experiment, we initiated oscillations by adding Sr^{2+} to the media of eggs expressing either FRESCA or CKAR, and then added GO6983 after ~90 min (Fig. S7). After GO6983 addition, the FRESCA response continues unabated in 100% of the eggs tested, whereas the CKAR response is attenuated in 60% of the eggs tested. This indicates that FRESCA is indeed reporting CaMKII activity in response to Sr^{2+}-induced oscillations.

We propose a molecular model to describe these data. Over the course of the first few Ca^{2+}/Sr^{2+} oscillations, the amplitude of the Rhod-2 signal is constant, whereas the FRESCA response and the Rhod-2 AUC increases from the first to the second rise (Fig. 6, *C–E*). Furthermore, once FRESCA signal peaks, it is sustained throughout the remainder of the data collection. This may suggest autophosphorylation of CaMKII at Thr-286, which facilitates activation at subsequent Ca^{2+} rises by increasing the affinity for Ca^{2+}/CaM (see cartoons in Fig. 6*A*) (32). Additionally, a prolonged time course of FRESCA response to Sr^{2+} indicates that FRESCA continues to faithfully track endogenous CaMKII up to 6 h (Fig. S8).

We generated a scrambled version of syntide and inserted this into the FRESCA construct to generate an unphosphorylatable variant. We expressed this sensor in eggs and added Sr^{2+} to initiate Ca^{2+} oscillations. The unphosphorylatable FRESCA did not respond to this stimulus, indicating that the signal change we observe using FRESCA is specific to a phosphorylation event (Fig. 6*F*).

Measuring CaMKII activity under native fertilization conditions

In mammals, fertilization-associated Ca^{2+} oscillations are induced by the release of sperm's phospholipase C ζ1 (PLCζ) into the ooplasm (47). We tested the response of both FRESCA and Camui in response to the expression of PLCζ.

Camui monitoring of PLCζ-induced Ca^{2+} oscillations

We assessed how Camui would report CaMKII activity induced by native Ca^{2+} oscillations and compared the response to those induced by Sr^{2+}. To do this, eggs expressing Camui were injected with PLCζ cRNA and Ca^{2+} and FRET responses were monitored (Fig. 7, *A* and *B*). We observed that Ca^{2+} oscillations nearly immediately induced CaMKII activity as monitored by Camui (Fig. 7*B*, *arrow* and *bottom inset*). However, this initial activity abruptly ceased and was not detected in subsequent rises. Only the first and second (and to a less extent, third) Ca^{2+} rises induced Camui responses despite the presence of robust and frequent Ca^{2+} oscillations (Fig. 7*A*). 75% of eggs (9/12) expressing Camui responded to the first or second Ca^{2+} rise. Additionally, despite the fact that the amplitude of the first Ca^{2+} rises remains relatively steady, the area under the curve showed a marked decrease after the second Ca^{2+} rise in these experiments (see Fig. 7, *E* and *J*). It is worth noting that the abundant expression of Camui may be contributing significantly to the existing CaMKII in the egg, and potentially altering Ca^{2+}/CaM dynamics. These results raised the possibility that Camui is not well-suited to detect CaMKII activity initiated by sporadic and low magnitude Ca^{2+} rises, which are characteristic of mammalian fertilization. Regardless, it remains to be elucidated why Sr^{2+}-induced oscillations are able to protractedly promote robust and persistent Camui responses, whereas the Camui response to PLCζ-induced oscillations fades rapidly.

FRESCA monitoring of PLCζ-induced Ca^{2+} oscillations

We injected PLCζ cRNA into FRESCA-expressing eggs, and thereafter began monitoring changes in FRESCA responses (Fig. 7, *F* and *G*). The initiation of oscillations stimulated the early activity of the endogenous CaMKIIγ, and this activity was detected with each additional rise. 100% of eggs (17/17) expressing FRESCA responded to the first or second Ca^{2+} rise. Similar to Sr^{2+}-induced oscillations, we observed a relative decrease in the amplitude of the Ca^{2+} rises over time, yet the FRESCA response was largely maintained (Fig. 7*G*). These observations are the longest evaluation of CaMKII activity reported following fertilization-like oscillations, as previous studies only reported up to 60 min post-initiation of oscillations (18, 23). These results also suggest that all Ca^{2+} rises induced by fertilization trigger activation of CaMKII (Fig. 7, *H–J*).

We tested the unphosphorylatable FRESCA variant in eggs injected with PLCζ cRNA. The unphosphorylatable FRESCA did not respond to this stimulus, indicating that the signal change we observe using FRESCA is specific to a phosphorylation event (Fig. 7*K*).

Finally, we compared the response of CKAR and FRESCA to PLCζ cRNA-induced oscillations. Side-by-side comparisons reveal delayed FRET changes for CKAR compared with

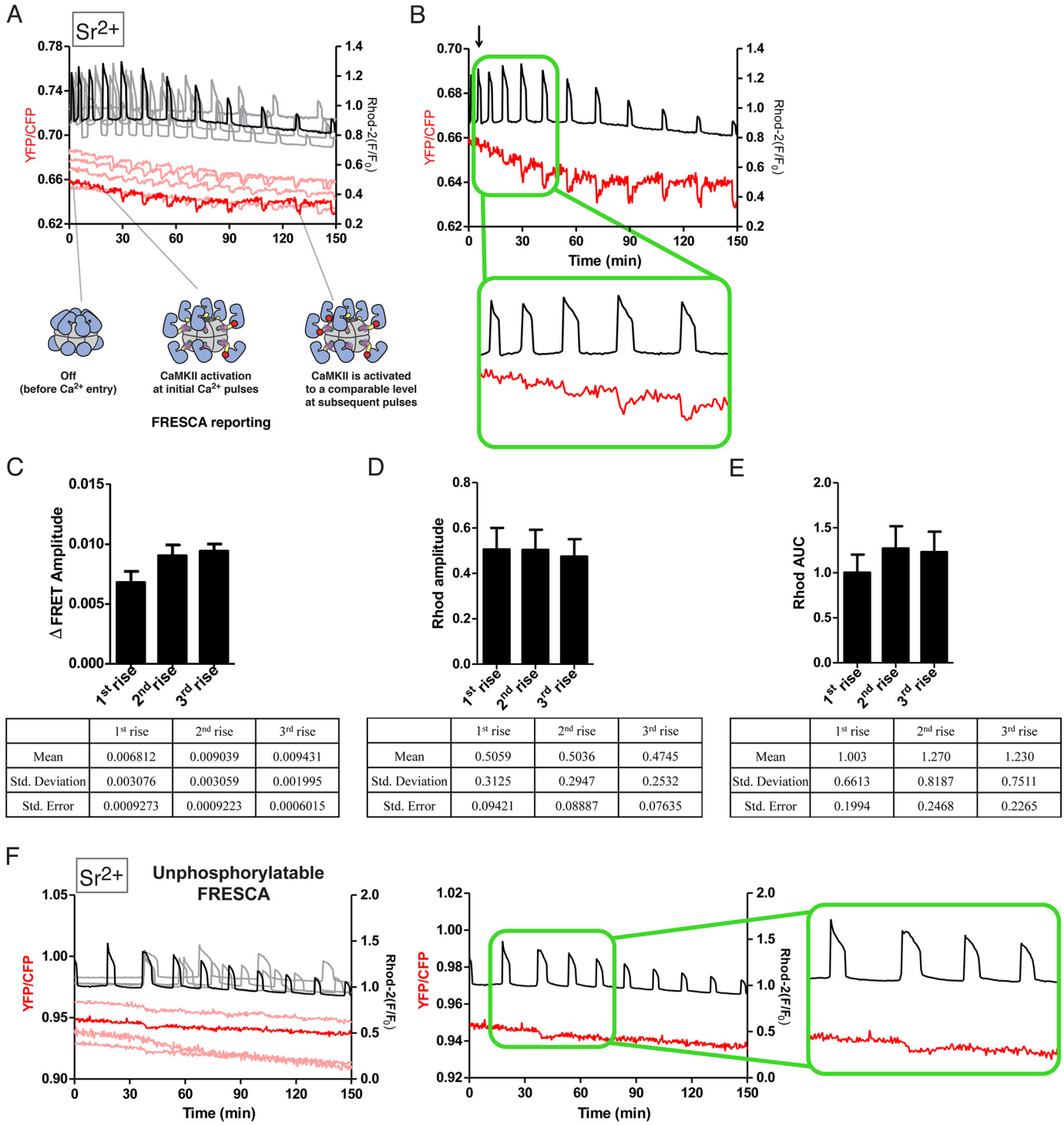

	1st rise	2nd rise	3rd rise
Mean	0.006812	0.009039	0.009431
Std. Deviation	0.003076	0.003059	0.001995
Std. Error	0.0009273	0.0009223	0.0006015

	1st rise	2nd rise	3rd rise
Mean	0.5059	0.5036	0.4745
Std. Deviation	0.3125	0.2947	0.2532
Std. Error	0.09421	0.08887	0.07635

	1st rise	2nd rise	3rd rise
Mean	1.003	1.270	1.230
Std. Deviation	0.6613	0.8187	0.7511
Std. Error	0.1994	0.2468	0.2265

Figure 6. Endogenous CaMKII activity tracks Ca^{2+} oscillations in mouse eggs. *A*, Ca^{2+} oscillations in eggs are induced by addition of Sr^{2+} to the extracellular media. Ca^{2+} is monitored by Rhod-2 (*black line*) and endogenous CaMKII activity is tracked by FRESCA (*red line*). *B*, one representative trace from Sr^{2+} oscillations is shown. *Inset* focuses on the first Ca^{2+} rises. *C–E*, three Ca^{2+} rises were quantified. The "1st rise" is that which induced the first FRET response, and then the subsequent 2 rises were measured. The ΔFRET amplitude (*C*), rhodamine amplitude (*D*), and rhodamine area under the curve (*E*) are shown. Statistics are reported in the tables *below*. 11 eggs over 2 replicates were used to generate the statistics. *F*, unphosphorylatable FRESCA contains a scrambled version of syntide that is not recognized by CaMKII. Multiple traces where Sr^{2+} was added are shown. A representative trace from each is shown to the *right*.

FRESCA (Fig. S9). These results are consistent with our observations following the addition of ionomycin (Fig. S6).

Discussion

It has been appreciated for decades that both Ca^{2+} oscillations and CaMKII activation in mouse eggs are crucial to fertilization and initiation of embryo development. Here, we provide an analysis of CaMKII activation in real-time in eggs using FRET-based CaMKII biosensors. Importantly, our new biosensor, FRESCA, allowed us to monitor endogenous CaMKII (CaMKIIγ3 and γJ) activity in real-time as a consequence of different activation stimuli (ionomycin, Sr^{2+}, and PLCζ). The

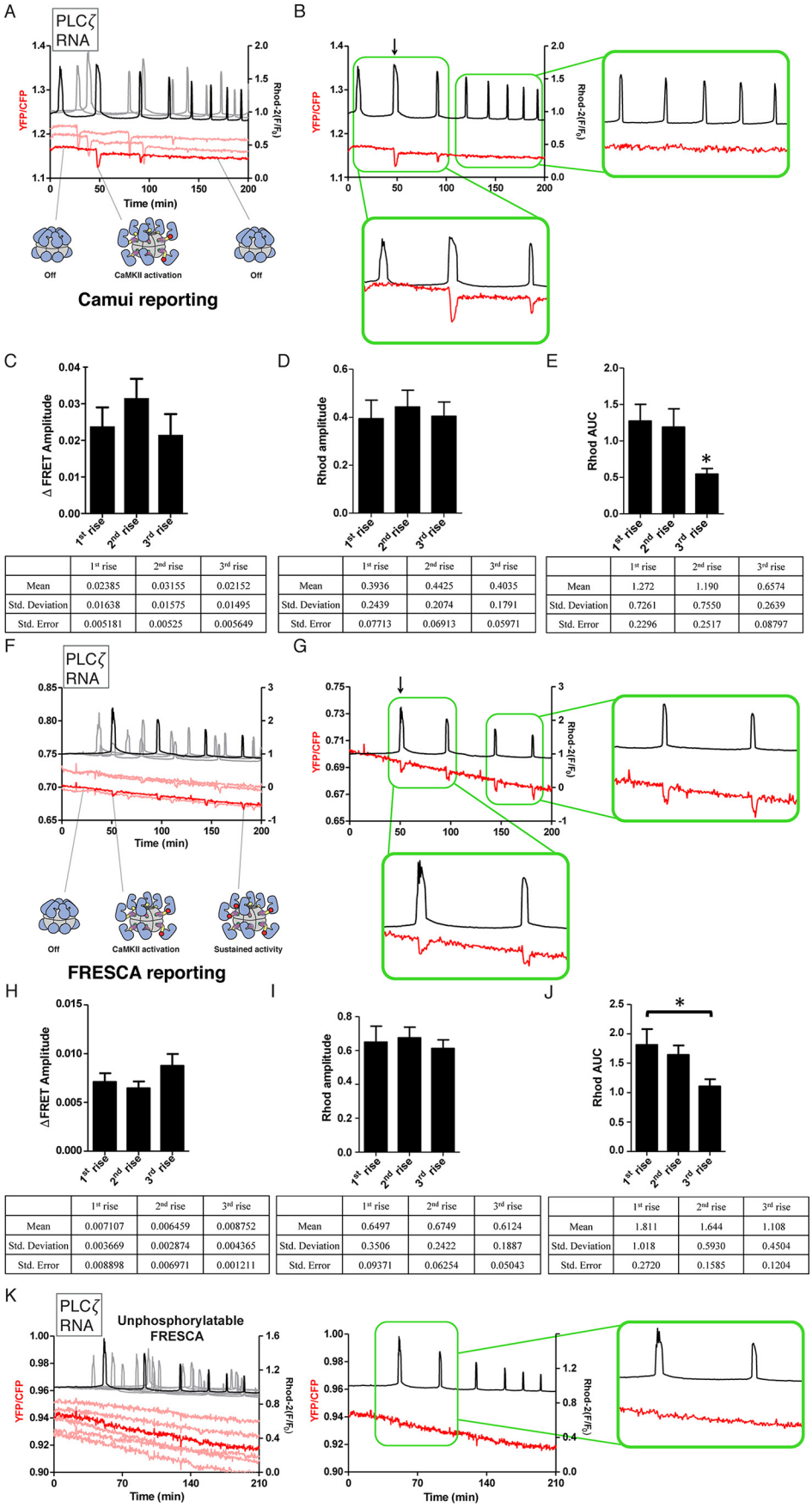

	1st rise	2nd rise	3rd rise
Mean	0.02385	0.03155	0.02152
Std. Deviation	0.01638	0.01575	0.01495
Std. Error	0.005181	0.00525	0.005649

	1st rise	2nd rise	3rd rise
Mean	0.3936	0.4425	0.4035
Std. Deviation	0.2439	0.2074	0.1791
Std. Error	0.07713	0.06913	0.05971

	1st rise	2nd rise	3rd rise
Mean	1.272	1.190	0.6574
Std. Deviation	0.7261	0.7550	0.2639
Std. Error	0.2296	0.2517	0.08797

	1st rise	2nd rise	3rd rise
Mean	0.007107	0.006459	0.008752
Std. Deviation	0.003669	0.002874	0.004365
Std. Error	0.008898	0.006971	0.001211

	1st rise	2nd rise	3rd rise
Mean	0.6497	0.6749	0.6124
Std. Deviation	0.3506	0.2422	0.1887
Std. Error	0.09371	0.06254	0.05043

	1st rise	2nd rise	3rd rise
Mean	1.811	1.644	1.108
Std. Deviation	1.018	0.5930	0.4504
Std. Error	0.2720	0.1585	0.1204

FRESCA response was noticeably different from Camui, which reports on the conformational change in the one CaMKII variant expressed in the sensor (in this paper and others, this variant is CaMKIIα). An additional advantage of FRESCA is that it does not alter the intracellular kinase concentrations, as already noted. When different Ca^{2+} oscillation patterns are induced, we observed subsequent differences in CaMKII activation in both sensors. From our data, it is clear that the (i) agent of Ca^{2+} oscillations, as well as the (ii) specific CaMKII isoform responding, both play a role in CaMKII activation.

The pivotal role of CaMKII activation in causing release of the meiotic arrest and initiation of embryonic development in all species was recently and more specifically evidenced by careful MS experiments (48). This study showed that soon after fertilization, and temporally coinciding with the Ca^{2+} wave, there is a strong increase in protein phosphorylation that far outweighs the biochemical changes caused by protein degradation that accompanies fertilization. Remarkably, the study also found that 25% of the phosphorylated sites matched the minimal phosphorylation motif of CaMKII. It is therefore important to determine how Ca^{2+} rises turn on CaMKII activity, and what parameter(s) of individual rises within an oscillatory pattern are necessary for periodic and consistent stimulation of its activity. We propose that the magnitude of the initial activation of CaMKII depends on the magnitude of the Ca^{2+} stimulus and on internal regulation of CaMKII. Knowing the minimal Ca^{2+} signal that increases the activity of CaMKIIγ is important, as we seek to develop more physiological methods of parthenogenetic activation to treat some cases of infertility.

Our data suggest that the endogenous CaMKIIγ in eggs is potentially more sensitive to Ca^{2+}/CaM than CaMKIIα. This finding is in line with previous data showing that longer linker CaMKII splice variants (CaMKIIγ3 and CaMKIIγJ) are activated at lower concentrations of Ca^{2+}/CaM than shorter linker variants (CaMKIIα) (see Fig. 1*E*) (8). Additionally, the delayed response seen in the Camui-expressing eggs in response to Sr^{2+} stimulation could also be a result of endogenous CaMKII being activated first (lower EC_{50} for Ca^{2+}/CaM) thereby competing with Camui for the available activating ligand.

Our study also represents the first characterization of the activation of CaMKII by a common parthenogenetic agonist in the mouse, such as Sr^{2+}. Although the FRESCA responses caused by Sr^{2+} and expression of PLCζ were similar in timing and persistence, the responses caused by these agonists following the expression of Camui were very different. Sr^{2+} oscillations induced delayed activation of Camui, but once it was activated, each Ca^{2+}/Sr^{2+} elevation resulted in successive Camui stimulation. Conversely, PLCζ-induced oscillations resulted in early activation of Camui followed by a rapid run down, such that after the second or third Ca^{2+} rise, and despite consistent Ca^{2+} oscillations, FRET changes in Camui were never again stimulated. These discrepancies likely have to do with the amplitude and/or duration of the Ca^{2+} rises induced by these two agonists. Learning the parameters of individual Ca^{2+} rises that are translated into endogenous CaMKII activity will be invaluable as we aim to design better parthenogenetic methods for application in IVF clinics.

Our results clearly show that the FRET changes reported by FRESCA significantly differ from that of CKAR, which reports on PKC activity. In addition to the effects of kinase-specific inhibitors and activators, there is a striking difference in the timing of response dynamics to all agonists examined here. This is consistent with previous reports showing CKAR responses in mouse eggs (46). It is not currently understood why CKAR oscillates persistently with Ca^{2+} release, as the reported predominant PKC isoform present in eggs is not directly activated by Ca^{2+}, and the Ca^{2+}-induced changes in diacylglycerol are expected to be minor (49, 50).

Addition of up to 10 μM ionomycin is a widely applied practice in IVF labs. Here, we showed that even a lower concentration range (0.5–5 μM ionomycin) results in substantially different activity profiles of CaMKII activation. With regard to the Camui experiments, in these FRET measurements we are observing direct activation of Camui (as opposed to endogenous CaMKII). It is clear that the extent of Camui activation depends on the amount of Camui present and the magnitude of the stimulus, as there is a significant increase in the amplitude of FRET change from 0.5 to 2.5 μM ionomycin. The FRESCA response (reporting on endogenous protein) at higher concentrations of ionomycin was more complex as it appears not to change significantly, which might reflect saturation of endogenous CaMKII or a negative feedback loop, as demonstrated by the transient nature of the maximal peak in FRESCA fluorescence change. These results indicate an unexpected effect on CaMKII activity even by increasing the ionomycin by 5-fold (2.5 μM), which will be crucial to elucidate further for clinical application.

More broadly, now that we have demonstrated the utility of FRESCA in mouse eggs, this opens the door to measuring endogenous CaMKII activity in other cell types, such as neurons and cardiomyocytes. Here, we thoroughly addressed the specificity of FRESCA in eggs, but this would need to be done in

Figure 7. FRESCA, but not Camui, continues to report CaMKII activation by Ca^{2+} oscillations induced by PLCζ. Ca^{2+} oscillations are induced by injection of PLCζ cRNA. CaMKII activity is monitored using FRESCA or Camui (FRET, *red lines*) and Ca^{2+} is monitored using Rhod-2 (*black lines*). *A*, an overlay of 3 representative eggs using Camui as the reporter of CaMKIIα activity. Cartoon depictions of hypothesized states of CaMKII are shown *below*. *Red circles* indicate Thr-286 phosphorylation. *B*, one representative trace from PLCζ-induced oscillations and Camui reporting is shown. *Insets* highlight the first and last pulses. *C–E*, quantification of Rhod-2 and FRET signals for Camui during PLCζ-induced Ca^{2+} rises. Three Ca^{2+} rises were quantified. The "1st rise" is that which induced the first FRET response, and then the subsequent 2 rises were measured. The ΔFRET amplitude (*C*), rhodamine amplitude (*D*), and rhodamine area under the curve (*E*) are shown. Statistics are reported in the tables *below*. Differences were considered significant at $p < 0.05$ (*) using one-way ANOVA. 12 eggs over 3 replicates were used to generate the statistics. Post hoc analyses were done using a Tukey multiple comparison test (Prism GraphPad). *F*, an overlay of 4 representative eggs using FRESCA as the reporter of endogenous CaMKII activity activity. *G*, one representative trace from PLCζ-induced oscillations and FRESCA reporting is shown. *Insets* highlight the first and last pulses. *H–J*, quantification of Rhod-2 and FRET signals for FRESCA during PLCζ-induced Ca^{2+} rises, as in *C–E*. The ΔFRET amplitude (*H*), rhodamine amplitude (*I*), and rhodamine area under the curve (*J*) are shown. Statistics are reported in the tables *below*. Differences were considered significant at $p < 0.05$ (*) using one-way ANOVA. Post hoc analyses were done using a Tukey multiple comparison test (Prism GraphPad). 17 eggs over 3 replicates were used to generate the statistics. *K*, unphosphorylatable FRESCA contains a scrambled version of syntide that is not recognized by CaMKII. Multiple traces where PLCζ cRNA was injected are shown. A representative trace from each is shown to the *right*.

other cell types as well. CaMKII activation has been heavily studied *in vitro* (8, 31, 51), and it is intriguing to also consider the potential effects of subunit exchange in cellular conditions (10, 52). It will be necessary to increase the signal to noise ratio of the FRESCA sensor to achieve a more robust signal for accurate quantification of kinetics and amplitudes. This should be possible by adjusting the length and/or rigidity of the linker regions in the sensor. Once this is accomplished, we believe that FRESCA will provide new insights into CaMKII activity in cells and allow us to further unravel the complexity of this unique protein kinase.

Experimental procedures

Plasmid design

To accommodate the requirements for FHA2 binding (53), syntide-2 was modified from PLARTLSVAGLPGKK to PLARALTVAGLPGKK to create syntide-FRESCA. Syntide-FRESCA was generated by annealing GATCCGGCGGCGCCGGCGGCGGCccgctggcgcgcgccctgaccgtggcgggcctgccgggcaaaaaaGGC and GGCCGCCttttttgcccggcaggcccgccacggtcagggcgcgcgccagcggGCCGCCGCCGGCGCCGCCG (IDT), which produced BamHI site at the 5′ end and a NotI site on the 3′ end. This product was phosphorylated (Ambion Inc.), purified (Thermo Fisher), and then ligated using T4 DNA ligase (Invitrogen) into a plasmid encoding the Aurora kinase FRET sensor (kind gift from Thomas Maresca). The final FRESCA sensor (with syntide-2 in place of the Aurora substrate) was cloned into pCDNA3.1. The unphosphorylatable FRESCA contains a scrambled version of syntide (RKVAAPKGAGLLLPA). We generated the scrambled sequence using an online tool: Mimitopes. This was cloned using the same technique as was used for cloning syntide-FRESCA.

Enzyme assays

Coupled-kinase assays were performed as previously described (31). Purified peptides (syntide-2 and syntide-FRESCA) were purchased from Lifetein (Somerset, NJ). Purified PKC was purchased from Promega (catalog number V5261). CaMKIIγ was expressed in Rosetta 2(DE3)pLysS-competent cells (Millipore) and purified as previously described (52). Fluorescence of NADH (excitation 340 nm/emission 460 nm) was monitored over time for 10 min using a Synergy H1 microplate reader (Biotek). For the experiments with syntide-2, the final enzyme concentration (both CaMKII and PKC) was 2.67 nM. For the experiments with syntide-FRESCA, the final enzyme concentration was 10 nM. CaMKIIγ activity was measured with the addition of 1 μM Ca^{2+}/CaM (activated) or an equivalent volume of buffer (control). Total CaMKII activity was corrected by subtracting the background rate without Ca^{2+}/CaM. PKC activity was measured with 1 mM Ca^{2+} and 140 μM/3.8 μM phosphatidylserine/diacylglycerol membranes (activated) or an equivalent volume of buffer (the protocol from Dr. Alexandra Newton's lab website was closely followed, modified from Ref. 54). The lipid mixture was prepared as follows: chloroform-solubilized lipids (Avanti) were mixed together at the appropriate ratio, dried under N_2, speed vacuumed for 1.5 h, and resuspended in 20 mM Hepes, pH 7.4, to make a ×10 solution. The mixture was vortexed and sonicated in a water bath for 30 s to fully resuspend. Rates were calculated as follows: first, the change in fluorescence over the time course was fit with a straight line ($y = mx + c$) to obtain a slope (m) proportional to the kinetic rate of the reaction. For each reaction, slopes were fit to a sliding window of 5 points (50 s) and the maximum observed slope was used to represent the kinetic rate. Total PKC activity was corrected by subtracting the background rate of all kinase assay components except for PKC to account for the contribution from lipid scattering. This rate was roughly equivalent to the background rate of PKC without addition of Ca^{2+}/lipid, but we only performed one subtraction. Total CaMKII activity was corrected by subtracting the background rate of all assay components except for Ca^{2+}/CaM.

HEK293T cell culture

All HEK293T cell cultures (kind gift from Dr. Daniel Hebert's lab) were grown in Dulbecco's modified Eagle's medium (Sigma) supplemented with 10% fetal bovine serum (Sigma) and maintained at 37 °C and 5% carbon dioxide levels. The identity of these cells was authenticated by ATCC using short tandem repeat analysis (CRL-3216 ATC 293T, lot 63226319). These cells tested negative for mycoplasma. Cells were transfected using Lipofectamine® 2000 Reagent (Invitrogen) and 150 ng of DNA constructs.

Collection of mouse eggs

MII eggs were collected from the oviducts of 6- to 10-week-old CD-1 female mice 12–14 h after administration of 5 IU of human chorionic gonadotropin (hCG), which was administered 46–48 h after the injection of 5 IU of pregnant mare serum gonadotropin (Sigma). Cumulus cells were removed with 0.1% bovine testes hyaluronidase (Sigma). MII eggs were placed in KSOM with amino acids (Millipore, Sigma) under mineral oil at 37 °C in a humidified atmosphere of 5% CO_2 until the time of monitoring. All animal procedures were performed according to research animal protocols approved by the University of Massachusetts Institutional Animal Care and Use Committee.

Preparation of cRNAs and microinjections

The sequences encoding Camui and FRESCA were subcloned into a pcDNA6 vector (pcDNA6/Myc-His B; Invitrogen) between the XhoI and PmeI restriction sites. Mouse PLCζ was a kind gift from Dr. K. Fukami (Tokyo University of Pharmacy and Life Science, Japan) and subcloned into a PCS2+ vector, as previously described by us (55). CKAR was ordered from Addgene (plasmid number 14860). Plasmids were linearized with a restriction enzyme downstream of the insert to be transcribed and cDNAs were *in vitro* transcribed using the T7 or SP6 mMESSAGE mMACHINE Kit (Ambion, Austin, TX) according to the promoter present in the construct. A poly(A)-tail was added to the mRNAs using a Tailing Kit (Ambion) and poly(A)-tailed RNAs were eluted with RNase-free water and stored in aliquots at −80 °C. Microinjections were performed as described previously (6). cRNAs were centrifuged, and the top 1–2 μl was used to prepare microdrops from which glass micropipettes were loaded by aspiration. cRNA (1 μg/μl) were delivered into eggs by pneumatic pressure (PLI-100 picoinjector, Harvard Apparatus, Cambridge, MA). Each egg received 5–10 pl, which is ~1–3% of the total volume of the egg. Injected

MII eggs were allowed for translation up to 4 h in KSOM. Groups of eggs were injected with mouse PLCζ cRNA after 4 h of FRET construct injection.

FRET and calcium imaging

To estimate relative changes in the cytoplasmic activity of Camui, FRESCA and/or CKAR, emission ratio imaging of the YFP/CFP was performed using a CFP excitation filter, dichroic beam splitter, CFP and YFP emission filters (Chroma technology, Rockingham, VT; ET436/20X, 89007bs, ET480/40m, and ET535/30m). To measure Camui and/or FRESCA activity and $[Ca^{2+}]_i$ simultaneously, eggs that had been injected with Camui and/or FRESCA cRNAs were loaded ~4 h post-injection with 1 μM Rhod-2AM supplemented with 0.02% pluronic acid for 20 min at room temperature. Eggs were then immobilized on glass-bottom dishes (MatTek Corp., Ashland, MA) by putting them in protein-free media (which causes the eggs to stick to the glass), and finally placed on the stage of an inverted microscope. CFP, YFP, and Rhod-2 intensities were collected every 20 s by a cooled Photometrics SenSys CCD camera (Roper Scientific, Tucson, AZ). The rotation of excitation and emission filter wheels was controlled using the MAC5000 filter wheel/shutter control box (Ludl) and NIS-elements software (Nikon). Imaging was performed on an inverted epifluorescence microscope (Nikon Eclipse TE 300, Analis Ghent, Belgium) using a ×20 objective. For studies where ionomycin was used to induce Ca^{2+} responses, eggs were transferred into a 360-μl Ca^{2+}-free TL-Hepes drop on a glass bottom dish, after which and following a brief monitoring period to determine baseline $[Ca^{2+}]_i$ values, different concentrations of ionomycin were added and Ca^{2+} responses monitored. For Sr^{2+} studies, eggs were transferred into a nominally Ca^{2+}-free TL-Hepes, containing 10 mM Sr^{2+}. In cases where $[Ca^{2+}]_i$ oscillations were induced by injection of PLCζ cRNA, eggs were placed in TL-Hepes media containing 2 mM Ca^{2+} within 20 min of the injection of PLCζ cRNA, which occurred 4 h post-injection of the FRET constructs (Camui or FRESCA).

Pharmacological tests in mouse eggs

Mouse eggs were transferred to Ca^{2+}-free TL-Hepes containing the desired concentrations of pharmacological compounds 5 min prior to Ca^{2+} imaging. FRET (YFP/CFP) was monitored simultaneously with Ca^{2+} (rhodamine signal). First, we determined how much inhibitor could be added without affecting Ca^{2+} entry. Concentrations of inhibitors were chosen based on this information as well as what was used in previous studies (see text for references). All media was Ca^{2+} free. The following concentrations and number of replicates were used: ionomycin/FRESCA (0.5 μM, $n = 18$), ionomycin/CKAR (0.5 μM, $n = 20$), ionomycin/GO6983/FRESCA (0.5/5 μM, $n = 14$), ionomycin/GO6983/CKAR (0.5/5 μM, $n = 15$), PMA/CKAR (1 μM, $n = 16$), PMA/FRESCA (1 μM, $n = 13$), Sr^{2+}/GO6983/FRESCA (10 mM/5 μM, $n = 9$), Sr^{2+}/GO6983/CKAR (10 mM/5 μM, $n = 7$), AS105 (5 μM, $n = 19$), and AS461 (5 μM, $n = 14$). AS105 (kind gift from Allosteros Therapeutics, Inc.) has not been used in mouse eggs, so we adjusted the concentration to a level where the Ca^{2+} release was not affected. Eggs with the first 4 compounds added were stimulated with 0.5 μM ionomycin, whereas the eggs with AS compounds were stimulated with 2.5 μM ionomycin. Side by side controls were performed under the same conditions (0.5 *versus* 2.5 μM ionomycin).

Confocal imaging

Confocal images were acquired using a Nikon Apo 1.4 NA ×60 oil immersion objective on a Nikon A1R confocal TiE microscope stand equipped with a LU-NV laser launch system and DU4 detector system housed in the IALS Nikon Center of Excellence microscopy facility at the University of Massachusetts, Amherst. The Galvano scanner was used and the pinhole size was set to 17.88 μm. CFP was excited with the 445-nm laser at 9.2%, 540/30 emission filter, and photomultiplier tube set to 75. YFP was excited with the 514 nm laser at 5.6%, 585/65 emission filter, and photomultiplier tube set to 58. Z-stacks images were collected at 1024 × 1024 in 12 bits and the step size was 1.00 μm.

Data processing and statistical analyses

Graphs reporting FRET changes and Ca^{2+} responses were prepared using the values of the YFP (436 × 535)/CFP (436 × 480) ratios on the left axis. No correction was applied here; just the raw ratios are plotted. Rhod-2 values were calculated using the following formula $(F)/F_0$ (actual value at × time/average baseline values for the first 2 min of monitoring) and the scale placed on the right axis. For calculation of time to FRET peak, analyses were performed in Excel to identify the baseline and highest or lowest value for each peak (Rhod-2 or FRET, respectively). For calculation of area under the curve and all statistics, we used Prism GraphPad. Values from three or more replicates were performed on different batches of eggs with at least 5 eggs per condition per replicate. These are presented as mean ± S.E. and were analyzed by ANOVA. Differences were considered significant at $p < 0.05$. Post hoc analyses were done using a Tukey multiple comparison test (Prism GraphPad).

Author contributions—G. A., M. C. W., T. J. M., R. A. F., and M. M. S. conceptualization; G. A., M. C. W., R. A. F., and M. M. S. data curation; G. A., M. C. W., R. A. F., and M. M. S. formal analysis; G. A. and M. C. W. validation; G. A., M. C. W., R. A. F., and M. M. S. investigation; G. A. and M. M. S. visualization; G. A., M. C. W., R. A. F., and M. M. S. methodology; G. A., R. A. F., and M. M. S. writing-original draft; G. A., M. C. W., R. A. F., and M. M. S. writing-review and editing; R. A. F. and M. M. S. resources; R. A. F. and M. M. S. supervision; R. A. F. and M. M. S. funding acquisition; R. A. F. and M. M. S. project administration.

Acknowledgments—We thank Changli He for assistance on RNA purification. The microscopy data were gathered in the Light Microscopy Facility and Nikon Center of Excellence at the Institute for Applied Life Sciences, University of Massachusetts, Amherst, with support from the Massachusetts Life Sciences Center. We thank Allosteros Therapeutics for providing AS105 and AS461, and Howard Schulman for helpful discussions. We thank members of the Stratton lab (Roman Sloutsky and Noelle Dziedzic) and Alejandro Heuck for assistance with reagents for the enzyme assays. We also thank Peter Chien, Eric Strieter, Scott Garman for discussions, and John Kuriyan for helpful comments on the manuscript.

References

1. Cuthbertson, K. S., Whittingham, D. G., and Cobbold, P. H. (1981) Free Ca^{2+} increases in exponential phases during mouse oocyte activation. *Nature* **294,** 754–757 CrossRef Medline
2. Swann, K., and Lai, F. A. (2013) PLCzeta and the initiation of Ca^{2+} oscillations in fertilizing mammalian eggs. *Cell Calcium* **53,** 55–62 CrossRef Medline
3. Eisner, D. A., Caldwell, J. L., Kistamás, K., and Trafford, A. W. (2017) Calcium and excitation-contraction coupling in the heart. *Circ. Res.* **121,** 181–195 CrossRef Medline
4. Rutecki, P. A. (1992) Neuronal excitability: voltage-dependent currents and synaptic transmission. *J. Clin. Neurophysiol.* **9,** 195–211 CrossRef Medline
5. Herring, B. E., and Nicoll, R. A. (2016) Long-term potentiation: from CaMKII to AMPA receptor trafficking. *Annu. Rev. Physiol.* **78,** 351–365 CrossRef Medline
6. Escoffier, J., Lee, H. C., Yassine, S., Zouari, R., Martinez, G., Karaouzène, T., Coutton, C., Kherraf, Z. E., Halouani, L., Triki, C., Nef, S., Thierry-Mieg, N., Savinov, S. N., Fissore, R., Ray, P. F., and Arnoult, C. (2016) Homozygous mutation of PLCZ1 leads to defective human oocyte activation and infertility that is not rescued by the WW-binding protein PAWP. *Hum. Mol. Genet.* **25,** 878–891 CrossRef Medline
7. Yoon, S. Y., Jellerette, T., Salicioni, A. M., Lee, H. C., Yoo, M. S., Coward, K., Parrington, J., Grow, D., Cibelli, J. B., Visconti, P. E., Mager, J., and Fissore, R. A. (2008) Human sperm devoid of PLC, ζ1 fail to induce Ca^{2+} release and are unable to initiate the first step of embryo development. *J. Clin. Invest.* **118,** 3671–3681 CrossRef Medline
8. Chao, L. H., Stratton, M. M., Lee, I. H., Rosenberg, O. S., Levitz, J., Mandell, D. J., Kortemme, T., Groves, J. T., Schulman, H., and Kuriyan, J. (2011) A mechanism for tunable autoinhibition in the structure of a human Ca^{2+}/calmodulin-dependent kinase II holoenzyme. *Cell* **146,** 732–745 CrossRef Medline
9. De Koninck, P., and Schulman, H. (1998) Sensitivity of CaM kinase II to the frequency of Ca^{2+} oscillations. *Science* **279,** 227–230 CrossRef Medline
10. Bhattacharyya, M., Stratton, M. M., Going, C. C., McSpadden, E. D., Huang, Y., Susa, A. C., Elleman, A., Cao, Y. M., Pappireddi, N., Burkhardt, P., Gee, C. L., Barros, T., Schulman, H., Williams, E. R., and Kuriyan, J. (2016) Molecular mechanism of activation-triggered subunit exchange in Ca/calmodulin-dependent protein kinase II. *eLife* **5,** e13405 CrossRef Medline
11. Rosenberg, O. S., Deindl, S., Comolli, L. R., Hoelz, A., Downing, K. H., Nairn, A. C., and Kuriyan, J. (2006) Oligomerization states of the association domain and the holoenzyme of Ca^{2+}/CaM kinase II. *FEBS J.* **273,** 682–694 CrossRef Medline
12. Lai, Y., Nairn, A. C., and Greengard, P. (1986) Autophosphorylation reversibly regulates the Ca^{2+}/calmodulin-dependence of Ca^{2+}/calmodulin-dependent protein kinase II. *Proc. Natl. Acad. Sci. U.S.A.* **83,** 4253–4257 CrossRef Medline
13. Miller, S. G., and Kennedy, M. B. (1986) Regulation of brain type II Ca^{2+}/calmodulin-dependent protein kinase by autophosphorylation: a Ca^{2+}-triggered molecular switch. *Cell* **44,** 861–870 CrossRef Medline
14. Wu, J. Q., and Kornbluth, S. (2008) Across the meiotic divide: CSF activity in the post-Emi2/XErp1 era. *J. Cell Sci.* **121,** 3509–3514 CrossRef Medline
15. Suzuki, M., Hara, Y., Takagi, C., Yamamoto, T. S., and Ueno, N. (2011) MID1 and MID2 are required for *Xenopus* neural tube closure through the regulation of microtubule organization (vol 137, pg 2329, 2010). *Development* **138,** 385–385 CrossRef
16. Miyazaki, S., Yuzaki, M., Nakada, K., Shirakawa, H., Nakanishi, S., Nakade, S., and Mikoshiba, K. (1992) Block of Ca^{2+} wave and Ca^{2+} oscillation by antibody to the inositol 1,4,5-trisphosphate receptor in fertilized hamster eggs. *Science* **257,** 251–255 CrossRef Medline
17. Ducibella, T., Huneau, D., Angelichio, E., Xu, Z., Schultz, R. M., Kopf, G. S., Fissore, R., Madoux, S., and Ozil, J. P. (2002) Egg-to-embryo transition is driven by differential responses to Ca^{2+} oscillation number. *Dev. Biol.* **250,** 280–291 CrossRef Medline
18. Ozil, J. P., Markoulaki, S., Toth, S., Matson, S., Banrezes, B., Knott, J. G., Schultz, R. M., Huneau, D., and Ducibella, T. (2005) Egg activation events are regulated by the duration of a sustained $[Ca^{2+}]$cyt signal in the mouse. *Dev. Biol.* **282,** 39–54 CrossRef Medline
19. Lorca, T., Cruzalegui, F. H., Fesquet, D., Cavadore, J. C., Méry, J., Means, A., and Dorée, M. (1993) Calmodulin-dependent protein kinase-Ii mediates inactivation of Mpf and Csf upon fertilization of *Xenopus* eggs. *Nature* **366,** 270–273 CrossRef Medline
20. Miao, Y. L., Stein, P., Jefferson, W. N., Padilla-Banks, E., and Williams, C. J. (2012) Calcium influx-mediated signaling is required for complete mouse egg activation. *Proc. Natl. Acad. Sci. U.S.A.* **109,** 4169–4174 CrossRef
21. Chang, H. Y., Minahan, K., Merriman, J. A., and Jones, K. T. (2009) Calmodulin-dependent protein kinase γ3 (CamKIIγ3) mediates the cell cycle resumption of metaphase II eggs in mouse. *Development* **136,** 4077–4081 CrossRef Medline
22. Ducibella, T., Schultz, R. M., and Ozil, J. P. (2006) Role of calcium signals in early development. *Semin. Cell Dev. Biol.* **17,** 324–332 Medline
23. Markoulaki, S., Matson, S., and Ducibella, T. (2004) Fertilization stimulates long-lasting oscillations of CaMKII activity in mouse eggs. *Dev. Biol.* **272,** 15–25 CrossRef Medline
24. Deguchi, R., Shirakawa, H., Oda, S., Mohri, T., and Miyazaki, S. (2000) Spatiotemporal analysis of Ca^{2+} waves in relation to the sperm entry site and animal-vegetal axis during Ca^{2+} oscillations in fertilized mouse eggs. *Dev. Biol.* **218,** 299–313 CrossRef Medline
25. Fissore, R. A., Dobrinsky, J. R., Balise, J. J., Duby, R. T., and Robl, J. M. (1992) Patterns of intracellular Ca^{2+} concentrations in fertilized bovine eggs. *Biol. Reprod.* **47,** 960–969 CrossRef Medline
26. Hatch, K. R., and Capco, D. G. (2001) Colocalization of CaM KII and MAP kinase on architectural elements of the mouse egg: potentiation of MAP kinase activity by CaM KII. *Mol. Reprod Dev.* **58,** 69–77 CrossRef Medline
27. Takao, K., Okamoto, K., Nakagawa, T., Neve, R. L., Nagai, T., Miyawaki, A., Hashikawa, T., Kobayashi, S., and Hayashi, Y. (2005) Visualization of synaptic Ca^{2+}/calmodulin-dependent protein kinase II activity in living neurons. *J. Neurosci.* **25,** 3107–3112 CrossRef Medline
28. Kline, D., and Kline, J. T. (1992) Repetitive calcium transients and the role of calcium in exocytosis and cell-cycle activation in the mouse egg. *Dev. Biol.* **149,** 80–89 CrossRef Medline
29. Bos-Mikich, A., and Whittingham, D. G. (1995) Analysis of the chromosome complement of frozen-thawed mouse oocytes after parthenogenetic activation. *Mol. Reprod. Dev.* **42,** 254–260 CrossRef Medline
30. Carvacho, I., Lee, H. C., Fissore, R. A., and Clapham, D. E. (2013) TRPV3 channels mediate strontium-induced mouse-egg activation. *Cell Rep.* **5,** 1375–1386 CrossRef Medline
31. Chao, L. H., Pellicena, P., Deindl, S., Barclay, L. A., Schulman, H., and Kuriyan, J. (2010) Intersubunit capture of regulatory segments is a component of cooperative CaMKII activation. *Nat. Struct. Mol. Biol.* **17,** 264–272 CrossRef Medline
32. Meyer, T., Hanson, P. I., Stryer, L., and Schulman, H. (1992) Calmodulin trapping by calcium-calmodulin-dependent protein kinase. *Science* **256,** 1199–1202 CrossRef Medline
33. Bayer, K. U., De Koninck, P., and Schulman, H. (2002) Alternative splicing modulates the frequency-dependent response of CaMKII to Ca^{2+} oscillations. *EMBO J.* **21,** 3590–3597 CrossRef Medline
34. Suzuki, T., Suzuki, E., Yoshida, N., Kubo, A., Li, H., Okuda, E., Amanai, M., and Perry, A. C. (2010) Mouse Emi2 as a distinctive regulatory hub in second meiotic metaphase. *Development* **137,** 3281–3291 CrossRef Medline
35. Violin, J. D., Zhang, J., Tsien, R. Y., and Newton, A. C. (2003) A genetically encoded fluorescent reporter reveals oscillatory phosphorylation by protein kinase C. *J. Cell Biol.* **161,** 899–909 CrossRef Medline
36. Liu, D., Vader, G., Vromans, M. J., Lampson, M. A., and Lens, S. M. (2009) Sensing chromosome bi-orientation by spatial separation of aurora B kinase from kinetochore substrates. *Science* **323,** 1350–1353 CrossRef Medline
37. Hashimoto, Y., and Soderling, T. R. (1987) Calcium. calmodulin-dependent protein kinase II and calcium: phospholipid-dependent protein kinase activities in rat tissues assayed with a synthetic peptide. *Arch. Biochem. Biophys.* **252,** 418–425 CrossRef Medline

38. Medvedev, S., Stein, P., and Schultz, R. M. (2014) Specificity of calcium/calmodulin-dependent protein kinases in mouse egg activation. *Cell Cycle* **13,** 1482–1488 CrossRef Medline
39. Wang, S. F., Kou, Z. H., Jing, Z. Y., Zhang, Y., Guo, X. Z., Dong, M. Q., Wilmut, I., and Gao, S. R. (2010) Proteome of mouse oocytes at different developmental stages. *Proc. Natl. Acad. Sci. U.S.A.* **107,** 17639–17644 CrossRef
40. Neef, S., Steffens, A., Pellicena, P., Mustroph, J., Lebek, S., Ort, K. R., Schulman, H., and Maier, L. S. (2018) Improvement of cardiomyocyte function by a novel pyrimidine-based CaMKII-inhibitor. *J. Mol. Cell. Cardiol.* **115,** 73–81 CrossRef Medline
41. Brooks, I. M., and Tavalin, S. J. (2011) Ca^{2+}/calmodulin-dependent protein kinase II inhibitors disrupt AKAP79-dependent PKC signaling to GluA1 AMPA receptors. *J. Biol. Chem.* **286,** 6697–6706 CrossRef Medline
42. Wong, M. H., Samal, A. B., Lee, M., Vlach, J., Novikov, N., Niedziela-Majka, A., Feng, J. Y., Koltun, D. O., Brendza, K. M., Kwon, H. J., Schultz, B. E., Sakowicz, R., Saad, J. S., and Papalia, G. A. (2019) The KN-93 molecule inhibits calcium/calmodulin-dependent protein kinase II (CaMKII) activity by binding to Ca^{2+}/CaM. *J. Mol. Biol.* **431,** 1440–1459 CrossRef Medline
43. Gou, X., Wang, W., Zou, S., Qi, Y., and Xu, Y. (2018) Protein kinase Cϵ mediates the inhibition of angiotensin II on the slowly activating delayed-rectifier potassium current through channel phosphorylation. *J. Mol. Cell. Cardiol.* **116,** 165–174 CrossRef Medline
44. Halet, G. (2004) PKC signaling at fertilization in mammalian eggs. *Biochim. Biophys. Acta* **1742,** 185–189 CrossRef Medline
45. Cuthbertson, K. S., and Cobbold, P. H. (1985) Phorbol ester and sperm activate mouse oocytes by inducing sustained oscillations in cell Ca^{2+}. *Nature* **316,** 541–542 CrossRef Medline
46. Gonzalez-Garcia, J. R., Machaty, Z., Lai, F. A., and Swann, K. (2013) The dynamics of PKC-induced phosphorylation triggered by Ca^{2+} oscillations in mouse eggs. *J. Cell. Physiol.* **228,** 110–119 CrossRef Medline
47. Saunders, C. M., Larman, M. G., Parrington, J., Cox, L. J., Royse, J., Blayney, L. M., Swann, K., and Lai, F. A. (2002) PLCζ: a sperm-specific trigger of Ca^{2+} oscillations in eggs and embryo development. *Development* **129,** 3533–3544 Medline
48. Presler, M., Van Itallie, E., Klein, A. M., Kunz, R., Coughlin, M. L., Peshkin, L., Gygi, S. P., Wühr, M., and Kirschner, M. W. (2017) Proteomics of phosphorylation and protein dynamics during fertilization and meiotic exit in the *Xenopus* egg. *Proc. Natl. Acad. Sci. U.S.A.* **114,** E10838–E10847 CrossRef Medline
49. Gangeswaran, R., and Jones, K. T. (1997) Unique protein kinase C profile in mouse oocytes: lack of calcium-dependent conventional isoforms suggested by rtPCR and Western blotting. *FEBS Lett.* **412,** 309–312 CrossRef Medline
50. Matsu-Ura, T., Shirakawa, H., Suzuki, K. G. N., Miyamoto, A., Sugiura, K., Michikawa, T., Kusumi, A., and Mikoshiba, K. (2019) Dual-FRET imaging of IP3 and Ca^{2+} revealed Ca^{2+}-induced IP3 production maintains long lasting Ca^{2+} oscillations in fertilized mouse eggs. *Sci. Rep.* **9,** 4829 CrossRef Medline
51. Rosenberg, O. S., Deindl, S., Sung, R. J., Nairn, A. C., and Kuriyan, J. (2005) Structure of the autoinhibited kinase domain of CaMKII and SAXS analysis of the holoenzyme. *Cell* **123,** 849–860 CrossRef Medline
52. Stratton, M., Lee, I. H., Bhattacharyya, M., Christensen, S. M., Chao, L. H., Schulman, H., Groves, J. T., and Kuriyan, J. (2014) Activation-triggered subunit exchange between CaMKII holoenzymes facilitates the spread of kinase activity. *eLife* **3,** e01610 CrossRef Medline
53. Durocher, D., Taylor, I. A., Sarbassova, D., Haire, L. F., Westcott, S. L., Jackson, S. P., Smerdon, S. J., and Yaffe, M. B. (2000) The molecular basis of FHA domain:phosphopeptide binding specificity and implications for phospho-dependent signaling mechanisms. *Mol. Cell* **6,** 1169–1182 CrossRef Medline
54. Kikkawa, U., Takai, Y., Minakuchi, R., Inohara, S., and Nishizuka, Y. (1982) Calcium-activated, phospholipid-dependent protein kinase from rat brain: subcellular distribution, purification, and properties. *J. Biol. Chem.* **257,** 13341–13348 Medline
55. Kurokawa, M., Yoon, S. Y., Alfandari, D., Fukami, K., Sato, K., Fissore, R. A. (2007) Proteolytic processing of phospholipase Czeta and [Ca2+]i oscillations during mammalian fertilization. *Dev Biol.* **312,** 407–418 CrossRef Medline